

Neural Network for Subgrid Turbulence Modeling for Large Eddy Simulations

Eduardo Vital^{a,*}, Jean-Marc Gratien^a, Yassine Ayoun^a, Thibault Faney^a and Julien Bohbot^a

^aIFP Energies nouvelles (IFPEN), 1-4 Av. du Bois Préau, 92852, Rueil-Malmaison, Île de France, France

ARTICLE INFO[†]

Keywords:

Data-driven closure models;
 Neural Networks;
 CFD

ABSTRACT

When simulating multiscale systems, where some fields cannot be fully prescribed despite their effects on the simulation's accuracy, closure models are needed. This behavior is observed in turbulent fluid dynamics, where Large Eddy Simulations (LES) depict global behavior while turbulence modeling introduces dissipation correspondent to smaller sub-grid scales. Recently, scientific machine learning techniques have emerged to address this problem by integrating traditional (physics-based) equations with data-driven (machine-learned) models, typically coupling numerical solvers with neural networks. This work presents a comprehensive workflow, encompassing high-fidelity data generation, a priori learning, and a posteriori learning, where data-driven models enhance differential equations. The study underscores the critical role of post-processing and effective filtering of fine-resolution fields and the implications numerical methods selection, such as the Lattice Boltzmann Method (LBM) or Finite Volume Method.

1. Introduction

Turbulence is a fundamental aspect of physical phenomena. Its inherently multiscale nature encompasses a vast spectrum of interacting ranges, posing significant challenges for accurate modeling.

In real-world applications, computational constraints prevent the resolution of small scales as achieved in Direct Numerical Simulation (DNS). Consequently, this unresolved dissipation must be modeled to account for their effects on larger-scale motions, as done in Large Eddy Simulations (LES) through closure models. The closure problem is ubiquitous in systems where macroscopic quantities of interest are significantly influenced by finer-scale dynamics.

In the generic context of multiscale problems described by Partial Differential Equations (PDEs), closure modeling can be systematically formalized as follows. Consider a typical PDE of the form $F(u, \mu) = 0$, where F is a differential operator, $u(x, t)$ the solution, and μ encompasses parameters such as boundary conditions and source terms. Methods aimed at mitigating the computational cost of solving such high-dimensional systems often involve approximating the solution $u(x, t)$ with a lower-dimensional counterpart \bar{u} , achieved through a reduction operator A : $u \mapsto \bar{u}$, representing convolution, projection, or similar techniques.

Thus, $\bar{u} \approx A(u)$. Correspondingly, the original system can be simplified as a reduced-order problem $\bar{F}(u, \mu)$, which serves as an approximation of the true solution u while being computationally more tractable to solve.

As the reduction step does not commute with the PDE operator, solving the reduced system demands: $\bar{F}(u, \mu) = A(F(u, \mu)) = F(\bar{u}, \mu) + C(u, \bar{u}, \mu) = 0$, where $C(u, \bar{u}, \mu)$ represents the closure term. In practice, C cannot be analytically determined from the differential equations, but rather depends on empirical models determined for the application in question.

In our work, we focus on the closure problem of turbulence within the field of Computational Fluid Dynamics (CFD). Here, u represents the velocity and pressure field solutions derived from governing equations, such as the Navier-Stokes (NS) or Boltzmann equations, which underpin the high-fidelity approach of Direct Numerical Simulations. In this context, the reduced model employed in Large Eddy Simulations for Navier-Stokes involves solving filtered equations supplemented by a closure component. This addition through a sub-grid scale (SGS) stress tensor τ_{ij} accounts for the effects of SGS dissipation, representing the turbulent energy dissipated by the unresolved small-scale eddies. Thus, the reduced NS system follows:

$$\frac{\partial \bar{u}}{\partial t} + \bar{u} \cdot \nabla \bar{u} = -\nabla \bar{p} + \nu \nabla^2 \bar{u} - \nabla \tau_{ij} \quad (1)$$

Over the years, a variety of models have been developed to approximate τ_{ij} - some relying on the Boussinesq hypothesis, which relates it to the strain rate tensor, like Smagorinsky, Dynamic Smagorinsky, and WALE; others

*Corresponding author

✉ eduardo.vital-brasil-lorenzo-fernandez@ifpen.fr (E. Vital); jean-marc.gratien@ifpen.fr (J. Gratien); yassine.ayoun@ifpen.fr (Y. Ayoun); thibault.faney@ifpen.fr (T. Faney); julien.bohbot@ifpen.fr (J. Bohbot)

ORCID(s): 0000-0001-6714-6774 (E. Vital); 0009-0005-5143-8082 (J. Gratien); 0009-0008-3448-6180 (Y. Ayoun); 0009-0005-8879-0012 (T. Faney); 0009-0002-0207-361X (J. Bohbot)

following structural or statistical approaches. [1, 2] provide an overview of both types.

Here, we propose a data-driven approach where the SGS stress tensor is computed using machine learning techniques. The closure problem is defined as a parameterized problem: $C_\theta(u, \bar{u}, \mu) = \bar{F}(u, \mu) - F(\bar{u}, \mu)$, where the learning process involves determining the optimal parameters θ that best fit the input-output pairs consisting of fine- and coarse-scale solutions obtained through post-processed DNS data. A neural network is trained on a dataset generated using the Taylor-Green Vortex (TGV) [3] test case (see Section 3.1). The performance of the model is evaluated both in a priori mode, using the generated dataset, and in a posteriori mode, where the closure model is integrated into an LES numerical solver.

The contribution of the paper is the implementation of an end-to-end workflow that not only addresses practical challenges in dataset generation but also bridges the gap between academic research and industrial practices, fostering a harmonious integration of both realms.

The paper is structured as follows: Section 2 reviews related works. Section 3 outlines the machine learning methodology we developed and implemented. Section 4 presents and discusses the results, and finally, Section 5 concludes the paper and suggests directions for future work.

2. Related works

The research for data-driven SGS turbulence modeling has been highly active in recent years, particularly with the integration of neural networks. In [4], the authors provide a review of recent contributions aligned with the closure equation formalism discussed in Section 1.

Typically, many of these contributions adopt a priori learning approaches [5, 6, 7, 8], which involve offline training of models by minimizing closure errors. However, these methods often face stability issues when applied in real-world scenarios, prompting studies such as [9, 10] to explore alternative strategies. Another avenue of research focuses on a posteriori learning [11, 12, 13], where models are trained by solving reduced equations and minimizing solution errors. Although this approach enhances stability, it incurs higher computational costs.

A third strategy involves hybrid methods, which blend a priori and a posteriori learning to strike a balance between performance and stability. Additionally, reconstruction techniques aim to recover high-dimensional solutions from reduced fields [14, 15, 16]. All these methods can be further enhanced by incorporating governing equations either as soft constraints, as demonstrated by Physics-Informed Neural Networks (PINNs) [17, 18], or as hard constraints, such as in Tensor-Basis Neural Networks (TBNNs), which enforce field invariance through symmetry [19, 20, 21].

3. Methodology

Our methodology falls under the a priori learning techniques discussed in Section 2. As it will be mentioned in Section 4, any possible stability issues occurring in a posteriori testing are yet to be analysed. According to the turbulence closure problem formalism introduced in Section 1, we employ **OpenLB** [22], a Lattice Boltzmann solver, as the DNS procedure. For the LES, we use the **OpenFOAM** [23] pimpleFoam solver to solve the incompressible Navier-Stokes equations. The closure problem is modeled as a parameterized problem: $C_\theta(u, \bar{u}, \mu) = \nabla \tau_{ij}$ where θ are the parameters of the neural network and:

$$\tau_{ij}(u, \bar{u}, \mu) = \overline{u_i u_j} - \bar{u}_i \bar{u}_j \quad (2)$$

In this section, we detail the dataset construction process and the reduction operator, outline the learning procedure, and discuss the techniques employed to integrate the trained model into the OpenFOAM LES solver.

3.1. Test Case and Simulations

As a starting point we proceed to generate a high-fidelity DNS of the 3d Taylor Green Vortex. This traditional, unsteady test case, is a classical academic experiment for turbulence analysis. It presents periodic boundary conditions distributed in the faces of a uniformly discretized cube, generating multiple turbulence scales in a highly anisotropic flow.

We choose to launch experiments at a moderate Reynolds number: 1600. In this way, we guarantee a complex, but yet stable, turbulent regime and a challenging task for the network. We also ensure a wide range of frequencies, enhancing the likelihood of generalization to lower frequencies in potential downstream testing.

To resolve all turbulence scales and account for dissipation from small eddies, we analyze the Kolmogorov length scale: $\eta = \left(\frac{v^3}{\epsilon} \right)^{1/4}$, where v is the kinematic viscosity, ϵ is the energy dissipation rate, and η the length scale equivalent to the mesh size. We conclude full DNS can be achieved a uniform discretization of the TGV at 512 resolution (512³ elements).

In addition, for purposes of validation and comparison, we launch both LBM and NS simulations using, respectively, OpenLB enhanced with CUDA and OpenFOAM multi-CPU. We plot on Figure 1 the effective dissipation curves for both during the initial 10 seconds and compare with the literature from Brachet [3]. We can deduce that our two DNS are equivalent.

For a posteriori testing and coupling, we stick to a Navier Stokes LES. The baseline for comparing the data-driven model is Smagorinsky, also plotted in Figure 1.

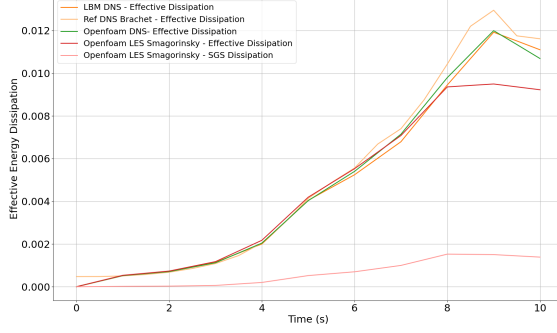


Figure 1: Effective energy dissipation per unit time for the original simulations - our two DNS (LBM and Navier Stokes), the DNS reference from Brachet, and our LES (Navier Stokes) with Smagorinsky turbulence modeling. For the latter, the dissipation due to the turbulence model is also plotted.

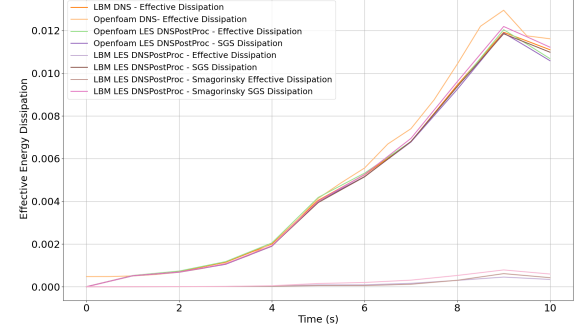


Figure 2: Effective energy dissipation per unit time for original and post-processed simulations - our two DNS (LBM and Navier Stokes) and the reduced simulations. The latter were achieved through a reduction operator $A : u \mapsto \bar{u}$ and include different turbulence models (Smagorinsky and 2), with their respective dissipation contributions also plotted.

3.2. Processing for Dataset Construction

Selecting the appropriate reduction operator $A : u \mapsto \bar{u}$ to obtain $\tau_{ij}(u, \bar{u}, \mu)$ from 2 is a non-trivial task, as in LES it is usually implicitly computed through the reduced equations 1. A common choice in literature is a mean convolution filter. For consistency with our a posteriori coupling, however, we opt for an explicit filter similar to the one in the Dynamic Smagorinsky implementation [24] for OpenFOAM. It performs a cell-to-node interpolation and averages the nodes in the same cell. This approach tends to benefit convergence in comparison to traditional convolutional filtering.

We further apply a deviatoric operation to τ_{ij} , i.e., $\tau_{ij}^d = \tau_{ij} - \frac{1}{3} \text{tr}(\tau_{ij}) \cdot \mathbf{I}$. In this way, we extract only the shear, anisotropic part of the tensor, removing the isotropic part that can be accounted by the pressure term in 1. A similar approach is done by [24] on the strain rate tensor S_{ij} .

Through the explicit reduction of the velocity, we can not only build the SGS stress tensor but also emulate the behavior of a lower-resolution LES. Figure 2 illustrates the effective energy dissipation of these processed DNS, transformed into LES. We treat both LBM and NS methods and compare equation 2 to the Smagorinsky model. We show that both approaches yield similar outcomes once again, and that Smagorinsky over-estimates the energy dissipation.

Finally, considering both OpenLB and OpenFOAM produce equivalent solutions, we select the former for training, due to its lower computational cost in this context.

3.3. Architecture and Learning Procedure

Between the mentioned networks on section 2, we choose, in a first moment, the simple architecture from [8]. It consists of a small MLP that performs pointwise inference on the fields, meaning it processes and predicts a single

tensor. Therefore, the rich input information of the gradient of the reduced field $\nabla \bar{u}$ with its 9 components is imputed and the symmetric SGS stress tensor (6 components) is outputted.

We perform, then, a priori training following the good practices of validation and hyperparameter optimization to find the best learning scheme, using a classical partition of 60-20-20 for train-test-validation. We propose a custom loss function, combining classical mean squared error (MSA) with the trace error of the symmetric SGS stress tensor: $\mathcal{L}_{\text{total}} = (1 - \alpha) \mathcal{L}_{\text{mse}} + \alpha \mathcal{L}_{\text{trace}}$, where α is used as a hyperparameter to be optimized.

As evaluation metric, we prefer a relative metric as the R2 score: $R_j^2 = 1 - \frac{\sum_{i=1}^N (T_j^{(i)} - \hat{T}_j^{(i)})^2}{\sum_{i=1}^N (T_j^{(i)} - \bar{T}_j)^2}$, where $\mathbf{T}^{(i)}$ and $\hat{\mathbf{T}}^{(i)}$ are, respectively, the predictions and the ground truth for the target tensor of the i_{th} point. We add the mean absolute error (MAE) to complement this metric: $\text{MAE}_j = \frac{1}{N} \sum_{i=1}^N |T_j^{(i)} - \hat{T}_j^{(i)}|$. The components j of the tensor can also be averaged to achieve a global metric.

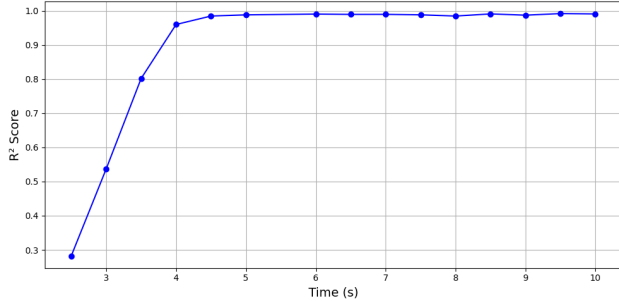
3.4. A Posteriori CFD-AI coupling

Finally, the model trained a priori is linked to a OpenFOAM LES. It is serialized and compiled with Pytorch, to be loaded by TorchLib in C++ and imported in a specially compiled version of the CFD software. We also implement an explicit SGS stress equation for turbulent dissipation of OpenFOAM, allowing to directly retrieve the model predictions.

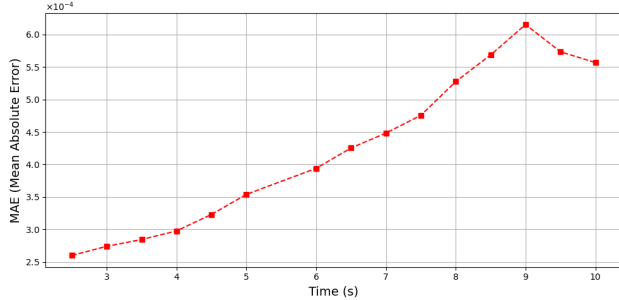
4. Experiments

We evaluate the capabilities of the model in different scenarios, ranging from time steps variations and subdomain separation. Sections 3.1 and 3.2 explained how the dataset was generated, while Section 3.3 described the partitioning, the learning scheme and the evaluation metrics employed throughout the experiments.

Figure 3 illustrates the a priori phase where the model, trained on the entire trajectory, performs on testing in the different time steps. The R² score approaches the unit from around 4 seconds onwards, coinciding with the development of a turbulent regime and increased dissipation (see Figure 1). Below this threshold, the flow is relatively laminar with lower dissipation, which leads to a degradation of the R² score.



(a) Evolution of R² score as a function of time



(b) Evolution of MAE as a function of time.

Figure 3: Evolution of error metrics over time in a priori, testing setting for the 10 seconds of the TGV experiment. The data originates from a LBM DNS, processed through a reduction operator $A : u \mapsto \bar{u}$.

The MAE provides complementary insight: the higher relative error at the early time window derives from the low magnitude of the target values, not poor model predictions. In fact, the absolute error remains low in this initial phase. Figure 4 further supports this, indicating that the norm of τ_{ij} is highly concentrated around zero early in the simulation, while it spreads to larger magnitudes later on.

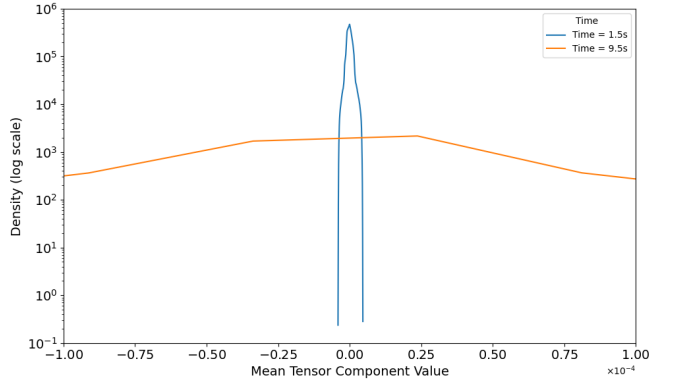


Figure 4: Comparison in logarithmic scale of the mean distribution of the SGS stress tensor components between an early stage (1.5 s) and a later stage (9.5 s) of the TGV simulation. The SGS stress tensor derives from a LBM DNS, processed through a reduction operator $A : u \mapsto \bar{u}$. The probability distribution curves are built from the histogram of samples from the testing set.

We also analysed how, if training on a single time step and on a subdomain of the whole cube (maintaining the same train-test-validation partitioning), the model would perform when testing on other time steps and parts of the domain. Remarkably, the network demonstrated excellent generalization capabilities, notably because it learned high-frequency features from the training set and inferred on lower frequencies. We refrain from including this analysis in this brief article, as well as the promising a posteriori testing, which requires further investigation.

5. Conclusions and Future Work

In this work, we present an end-to-end application for developing a data-driven closure model for turbulence in Large Eddy Simulations. We address practical questions arising during dataset generation and combine academical research with industrial practices to enrich the workflow.

The shortcomings of the present research will be investigated in future work. We recognize the limitations stemming from using a pointwise model. Thus, we intend to implement and test multi-hierarchical approaches such as GNNs and CNNs. Moreover, the inherent generalisation deficiency of standard neural networks signalizes the importance of more robust approaches - neural operators for space and time discretization invariance, as well as physically informed techniques for extrapolation to unknown frequencies and test cases. A robust set of experiments and ablation studies, guided by a posteriori performance, enlightens a promising direction.

References

- [1] S. B. Pope, Turbulent flows, *Measurement Science and Technology* 12 (11) (2001) 2020–2021.
- [2] I. Yilmaz, L. Davidson, Comparison of sgs models in large-eddy simulation for transition to turbulence in taylor-green flow, 2015.
- [3] M. E. Brachet, D. I. Meiron, S. A. Orszag, B. G. Nickel, R. H. Morf, U. Frisch, Small-scale structure of the taylor–green vortex, *Journal of Fluid Mechanics* 130 (1983) 411–452. doi: [10.1017/S0022112083001159](https://doi.org/10.1017/S0022112083001159).
- [4] B. Sanderse, P. Stinis, R. Maulik, S. E. Ahmed, Scientific machine learning for closure models in multiscale problems: A review, *arXiv preprint arXiv:2403.02913* (2024).
- [5] T. Dai, S. Liu, J. Liu, N. Jiang, Q. Chen, Development of a new dynamic smagorinsky model by an artificial neural network for prediction of outdoor airflow and pollutant dispersion, *Building and Environment* 243 (2023) 110624.
- [6] C. Yu, Z. Yuan, H. Qi, J. Wang, X. Li, S. Chen, Kinetic-energy-flux-constrained model using an artificial neural network for large-eddy simulation of compressible wall-bounded turbulence, *Journal of Fluid Mechanics* 932 (2022) A23.
- [7] M. Kurz, A. Beck, A machine learning framework for les closure terms, *ETNA - Electronic Transactions on Numerical Analysis* 56 (2022) 117–137. doi: [10.1553/etna_vol56s117](https://doi.org/10.1553/etna_vol56s117).
- [8] M. Kim, J. Park, H. Choi, Large eddy simulation of flow over a circular cylinder with a neural-network-based subgrid-scale model, *Journal of Fluid Mechanics* 984 (2024) A6. doi: [10.1017/jfm.2024.154](https://doi.org/10.1017/jfm.2024.154).
- [9] J. Park, H. Choi, Toward neural-network-based large eddy simulation: application to turbulent channel flow, *Journal of Fluid Mechanics* 914 (2021) A16. doi: [10.1017/jfm.2020.931](https://doi.org/10.1017/jfm.2020.931).
- [10] A. Beck, D. Flad, C.-D. Munz, Deep neural networks for data-driven les closure models, *Journal of Computational Physics* 398 (2019) 108910. doi: <https://doi.org/10.1016/j.jcp.2019.108910>.
- [11] H. Kim, V. Shankar, V. Viswanathan, R. Maulik, Generalizable data-driven turbulence closure modeling on unstructured grids with differentiable physics (2024). arXiv:2307.13533.
- [12] B. List, L.-W. Chen, N. Thuerey, Learned turbulence modelling with differentiable fluid solvers: physics-based loss functions and optimisation horizons, *Journal of Fluid Mechanics* 949 (Sep. 2022). doi: [10.1017/jfm.2022.738](https://doi.org/10.1017/jfm.2022.738).
- [13] A. Beck, M. Kurz, A perspective on machine learning methods in turbulence modeling, *GAMM-Mitteilungen* 44 (1) (Mar. 2021). doi: [10.1002/gamm.202100002](https://doi.org/10.1002/gamm.202100002).
- [14] L. Nista, C. D. Schumann, P. Petkov, V. Pavlov, T. Grenga, J. F. MacArt, A. Attili, S. Markov, H. Pitsch, Parallel implementation and performance of super-resolution generative adversarial network turbulence models for large-eddy simulation, *Computers & Fluids* 288 (2025) 106498. doi: <https://doi.org/10.1016/j.compfluid.2024.106498>.
- [15] K. Fukami, K. Fukagata, K. Taira, Machine-learning-based spatio-temporal super resolution reconstruction of turbulent flows, *Journal of Fluid Mechanics* 909 (Dec. 2020). doi: [10.1017/jfm.2020.948](https://doi.org/10.1017/jfm.2020.948).
- [16] Z. Yuan, C. Xie, J. Wang, Deconvolutional artificial neural network models for large eddy simulation of turbulence, *Physics of Fluids* 32 (11) (Nov. 2020). doi: [10.1063/5.0027146](https://doi.org/10.1063/5.0027146).
- [17] S. Cuomo, V. S. di Cola, F. Giampaolo, G. Rozza, M. Raissi, F. Piccialli, Scientific machine learning through physics-informed neural networks: Where we are and what's next (2022). arXiv:2201.05624.
- [18] M. Raissi, P. Perdikaris, G. E. Karniadakis, Physics informed deep learning (part i): Data-driven solutions of nonlinear partial differential equations (2017). arXiv:1711.10561.
- [19] J. Ling, R. Jones, J. Templeton, Machine learning strategies for systems with invariance properties, *Journal of Computational Physics* 318 (2016) 22–35. doi: <https://doi.org/10.1016/j.jcp.2016.05.003>.
- [20] J.-L. Wu, H. Xiao, E. Paterson, Physics-informed machine learning approach for augmenting turbulence models: A comprehensive framework, *Physical Review Fluids* 3 (7) (Jul. 2018). doi: [10.1103/physrevfluids.3.074602](https://doi.org/10.1103/physrevfluids.3.074602).
- [21] R. Bose, A. M. Roy, Invariance embedded physics-infused deep neural network-based sub-grid scale models for turbulent flows, *Engineering Applications of Artificial Intelligence* 128 (2024) 107483. doi: <https://doi.org/10.1016/j.engappai.2023.107483>.
- [22] V. Heuveline, J. Latt, The openlb project: an open source and object oriented implementation of lattice boltzmann methods, *International Journal of Modern Physics C* 18 (04) (2007) 627–634.
- [23] G. Chen, Q. Xiong, P. J. Morris, E. G. Paterson, A. Sergeev, Y. Wang, Openfoam for computational fluid dynamics, *Notices of the AMS* 61 (4) (2014) 354–363.
- [24] A. Passalacqua, Albertopa/dynamicsmagorinsky: dynamicsmagorinsky for openfoam 2.3.x (Apr. 2021). doi: [10.5281/zenodo.4697995](https://zenodo.4697995).